

***In vitro* metabolism of the synthetic cannabinoid 3,5-AB-CHMFUPPYCA and its 5,3-regioisomer and investigation of their thermal stability**

Florian Franz^{1,2}, Verena Angerer^{1,2}, Simon D. Brandt³, Gavin McLaughlin^{4,5}, Pierce V. Kavanagh⁵, Bjoern Moosmann¹, and Volker Auwärter^{1*}

¹ Institute of Forensic Medicine, Forensic Toxicology Department, Medical Center – University Freiburg, Albertstr. 9, 79104 Freiburg, Germany

² Hermann Staudinger Graduate School, University of Freiburg, Hebelstr. 27, 79104 Freiburg, Germany

³ School of Pharmacy and Biomolecular Sciences, Liverpool John Moores University, Byrom Street, Liverpool L3 3AF, UK

⁴ Department of Life and Physical Sciences, School of Science, Athlone Institute of Technology, Dublin Road, Athlone, Co. Westmeath, Ireland

⁵ Department of Pharmacology and Therapeutics, School of Medicine, Trinity Centre for Health Sciences, St. James's Hospital, Dublin 8, Ireland

* Corresponding author:

V. Auwärter

tel.: +49 761 203 6862

fax: +49 761 203 6826

e-mail: volker.auwaerter@uniklinik-freiburg.de

Abstract

Recently, the pyrazole-containing synthetic cannabinoid (SC) *N*-(1-amino-3-methyl-1-oxobutan-2-yl)-1-(cyclohexylmethyl)-3-(4-fluorophenyl)-1*H*-pyrazole-5-carboxamide (3,5-AB-CHMFUPPYCA) has been identified as a 'research chemical' both in powdered form and as an adulterant present in herbal preparations. Urine is the most common matrix used for abstinence control and the extensive metabolism of SCs requires implementation of targeted analysis. The present study describes the investigation of the *in vitro* phase I metabolism of 3,5-AB-CHMFUPPYCA and its regioisomer 5,3-AB-CHMFUPPYCA using pooled human liver microsomes. Metabolic patterns of both AB-CHMFUPPYCA isomers were qualitatively similar and dominated by oxidation of the cyclohexylmethyl side chain. Biotransformation to monohydroxylated metabolites of high abundance confirmed that these species might serve as suitable targets for urine analysis. Furthermore, since SCs are commonly administered by smoking and because some metabolites can also be formed as thermolytic artefacts, the stability of both isomers was assessed under smoking conditions. Under these conditions, pyrolytic cleavage of the amide bond occurred that led to approximately 3 % conversion to heat-induced degradation products that were also detected during metabolism. These artefactual 'metabolites' could potentially bias *in vivo* metabolic profiles after smoking and might have to be considered for interpretation of metabolite findings during hair analysis. This might be relevant in the analysis of hair samples where detection of metabolites is generally accepted as a strong indication of drug use rather than a potential external contamination.

Keywords: LC-MS/MS; metabolism; new psychoactive substances; pooled human liver microsomes; synthetic cannabinoids

Introduction

Cannabinoid receptor agonists, commonly referred to as synthetic cannabinoids, are the predominant class within the group of new psychoactive substances (NPS) with over 150 distinct structures reported via the European Early Warning System (EWS) to the European Monitoring Centre for Drugs and Drug Addiction (EMCDDA) until October 2015^[1]. Over the last seven years, the synthetic cannabinoids offered for purchase have undergone significant structural changes. While in the beginning mostly N-alkyl substituted naphthoylindoles were sold (e.g. JWH-018, JWH-210 and AM-2201), the majority of the synthetic cannabinoids offered in 2015 contain either indole or indazole core structures along with valinamide, methyl-valinamide or methyl ester variants of these structures (e.g. MDMB-CHMICA, AB-FUBINACA, AB-CHMINACA). Recently, three different synthetic cannabinoids comprising a pyrazole core structure were identified on the ‘legal high’ market (Figure 1). Girreser et al. reported the identification of the designer drug 3,5-5F-ADB-FUPPYCA (*N*-(1-amino-3,3-dimethyl-1-oxobutan-2-yl)-1-(5-fluoropentyl)-3-(4-fluorophenyl)-pyrazole-5-carboxamide)^[2] and McLaughlin et al. identified 3,5-AB-CHMFUPPYCA (*N*-(1-amino-3-methyl-1-oxobutan-2-yl)-1-(cyclohexylmethyl)-3-(4-fluorophenyl)-1*H*-pyrazole-5-carboxamide) in a powder falsely classified as AZ-037 (5F-AB-FUPPYCA^[3], *N*-(1-amino-3-methyl-1-oxobutan-2-yl)-1-(5-fluoropentyl)-5-(4-fluorophenyl)-1*H*-pyrazole-3-carboxamide), a compound which was itself reported through the EWS in June 2015^[1]. Uchiyama et al. also detected 3,5-AB-CHMFUPPYCA in an ‘herbal mixture’ sold in Japan and referred to it, following a semi-systematic nomenclature naming approach, as AB-CHFUPPYCA^[4]. Apart from the three pyrazole compounds identified on the drug market, the synthesis of the 5,3-regioisomer of 3,5-AB-CHMFUPPYCA was also described in the literature^[3]. No pharmacological data regarding these novel compounds is available so far. As many pyrazole compounds like rimonabant (SR141716A) bind to the CB₁ receptor as an antagonist, while some pyrrole compounds like JWH-307 show agonist properties with a high CB₁ binding affinity^[5], collection of such data would be of high interest. Even without this data, the appearance of these compounds on the ‘legal high’ market render it likely that these compounds may be capable of producing cannabis-like effects and show potential for misuse.

Offering a non-invasive sample collection with a relatively wide window of detection, urine analysis is usually the method of choice for abstinence control. In the case of synthetic cannabinoids, the parent compounds are rarely excreted unchanged in urine and in most cases, after cleavage with glucuronidase, the phase I main metabolites are suitable target analytes^[6-9]. Consequently, the metabolism of a new synthetic cannabinoid needs to be known prior to updating analytical methods. In cases where no authentic human sample material with confirmed uptake of the particular compound is available, pooled human liver microsomes (pHLM) offer an inexpensive and fast alternative to gain preliminary data on phase I metabolites to be expected. Furthermore, the pHLM extracts can be used for LC-MS/MS method development.

The present study describes the investigation of the *in vitro* phase I metabolites of 3,5-AB-CHMFUPPYCA and 5,3-AB-CHMFUPPYCA using pHLM. Since synthetic cannabinoids are commonly administered by smoking, the thermolytic stability of both isomers was also assessed under smoking conditions as some of the metabolites of synthetic

cannabinoids can also be formed as artefacts^[10], which can be of particular importance in terms of hair analysis.

Experimental

Chemicals and reagents

Formic acid (Rotipuran[®] $\geq 98\%$, p.a.), potassium hydrogen phosphate ($\geq 99\%$, p.a.) and 2-propanol (Rotisol[®] $\geq 99,95\%$, LC-MS grade) were obtained from Carl Roth (Karlsruhe, Germany), acetone, acetonitrile (ACN) (LC-MS grade), ammonium formate 10 M (99,995%), potassium hydroxide (puriss. p.a. $\geq 86\%$ (T) pellets) and superoxide dismutase (from bovine erythrocytes) from Sigma-Aldrich (Steinheim, Germany), and methanol from VWR (Darmstadt, Germany). Pooled human liver microsomes (pHLM) (50 Donors), NADPH-regenerating solutions A/B and 0.5 M potassium phosphate buffer pH 7.4 were purchased from Corning (New York, USA). 3,5-AB-CHMFUPPYCA and 5,3-AB-CHMFUPPYCA were synthesized as described elsewhere^[3]. Damiana leaves (*Turnera diffusa* Willd. ex Schult) were purchased from an online vendor (Krautrausch, Berlin, Germany). Deionized water was prepared using a cartridge deionizer from Memtech (Moorenweis, Germany). For LC-MS/MS analysis mobile phase A consisted of 1% ACN, 0.1% HCOOH, and 2 mM NH₄⁺HCOO⁻ in water, while mobile phase B consisted of ACN with 0.1% HCOOH, and 2 mM NH₄⁺HCOO⁻.

Identification of the *in vitro* metabolites (pHLM-Assay)

To investigate the phase I metabolism of 3,5-AB-CHMFUPPYCA and 5,3-AB-CHMFUPPYCA, *in vitro* experiments with pooled human liver microsomes (pHLM) were performed in triplicates. Each compound solution (0.5 μ L, 1 mg/mL) was added to 49.5 μ L of the pHLM (1 mg/mL) reaction mixture consisting of water, potassium phosphate buffer, superoxide dismutase, NADPH-regenerating solutions A/B and pHLM prior to incubation for 60 min at 37 °C. The reaction was terminated by the addition of ice-cold acetonitrile and the supernatant was analyzed after centrifugation and 1:10 dilution. Blank pHLM samples, used as negative controls were processed in the same way. The dilutions of the pHLM extracts were screened for potential metabolites applying LC-MS/MS precursor ion (Prec) scan, enhanced product ion (EPI) scan, and multiple reaction monitoring (MRM) experiments. For precursor ion scan experiments the characteristic fragment ion *m/z* 189 of 3,5-AB-CHMFUPPYCA and its 5,3 isomer (Supplemental Figure S1) was used to screen for metabolites. In case of the EPI scan experiments, all detected precursor masses and other predicted *m/z* values of potential phase I metabolites comprising mono-, di- and trihydroxylation, demethylation, dehalogenation, methylation, carboxylation, amide cleavage, dehydrogenation, dealkylation, dihydrodiol formation and ketone formation were included as well as combinations of the potential metabolic modifications. Specific mass transitions of the identified metabolite showing the most abundant signals were included in a MRM method used for abstinence control in urine samples (Supplemental Tables S1 and S2).

LC-MS/MS analysis

The LC-MS/MS system consisted of an Nexera X2 UHPLC (Shimadzu, Duisburg, Germany) coupled to a QTRAPTM 5500 triple quadrupole linear ion trap instrument (SCIEX, Darmstadt, Germany). Chromatographic separation was performed on a Kinetex[®] C₁₈ column (2.6 μm, 100 Å, 100×2.1 mm; Phenomenex, Aschaffenburg, Germany) applying gradient elution as follows: starting concentration of mobile phase B was 10 % held for 0.3 min, increased to 20 % at 0.5 min, further increased to 55 % at 20.0 min, further increased to 95 % at 20.1 min, held until 21.9 min, decreased to starting conditions of 10 % at 22.0 min and held 3.0 min for equilibration. The flow rate was set to 0.3 mL/min and the autosampler as well as the column oven temperatures were set to 10 and 40 °C, respectively. Declustering potentials, entrance potentials, collision energies and cell exit potentials were optimized for the two parent compounds (Supplemental Table S1 and S2). Ion source temperature and ion source voltage were set at 600 °C and +5500 V, respectively. Curtain gas (N₂) pressure was 35 psi, ion source gas 1 and 2 (compressed air) pressure were 50 and 60 psi and collision gas (N₂) pressure was set to 'high'.

Smoke condensate

To investigate the pyrolytic stability of 3,5-AB-CHMFUPPYCA and its 5,3-isomer during smoking, three different joints were prepared. One joint consisted solely of 300 mg dried damiana plant material and served as a blank control. The other two joints were prepared with 300 mg damiana which was sprayed with one milliliter of an acetone solution of 3.5 mg/mL 3,5-AB-CHMFUPPYCA or 5,3-AB-CHMFUPPYCA, respectively. After air drying overnight, the fortified plant material was rolled in a joint. The joints were burned down in about 2 min using a water jet pump while the smoke was directed through a wash bottle filled with 100 mL methanol. A 0.5 mL aliquot of each smoke condensate solution was evaporated to dryness under a gentle stream of nitrogen at 40 °C and reconstituted in 0.5 mL ethyl acetate prior to analysis with a GC-MS screening method described elsewhere^[11]. Another aliquot was reconstituted in mobile phase A/B (50/50, Vol.-%) for LC-MS/MS analysis.

Results and discussion

Identification of the main metabolites

In total, 22 metabolites of 3,5-AB-CHMFUPPYCA, the isomer offered via the Internet and found in a 'herbal mixture' in Japan, could be detected in the pHLM assay (Table 1). The four most abundant metabolites were all products of monohydroxylation at the cyclohexylmethyl moiety (A08, A09, A10 and A11). The EPI spectra of these metabolites are shown in Figure 2.

In case of the regioisomer 5,3-AB-CHMFUPPYCA, 23 metabolites were identified in the pHLM assay (Table 2). Similar to the 3,5-isomer, the preferred site of oxidative biotransformation was the cyclohexylmethyl moiety, leading to three hydroxylation products (B06, B13 and B08) and one ketone (B12) as the most abundant metabolites. The EPI spectra of these four metabolites are shown in Figure 3. The ranking is solely based on the area ratios (metabolite/most abundant metabolite) and does not necessarily reflect actual concentrations. This is mainly due to the fact that differences in ionization efficiencies may significantly bias

abundance while matrix effects seem to be negligible in pHLM assays with synthetic cannabinoids (own unpublished data).

When comparing the metabolite profiles of the two isomers, 5,3-AB-CHMFUPPYCA appeared to be more efficiently metabolized enzymatically under the chosen conditions. Supplemental Figure S2 shows exemplary chromatograms for both compounds with a higher signal for the unchanged 3,5-AB-CHMFUPPYCA. The metabolites of the two isomers can be differentiated by monitoring the transition to m/z 260 as this fragment seemed to be unique to the 3,5-substituted compounds. Differentiation might be of interest because the two isomers could show different pharmacological activity and could differ with regard to their legal status.

In vitro findings do not necessarily correlate with *in vivo* findings, particularly in terms of the ranking regarding relative abundance. Moreover, differences in the relative abundance of metabolites might be expected depending on individual phenotype, dose and time of last intake. However, taking into account the available data regarding human metabolic transformation of chemically related compounds, it is very likely that hydroxylation at the cyclohexylmethyl moiety will be among the main metabolic reactions.

Thermolytic stability under smoking conditions

Analysis of the pHLM extracts highlighted the elimination of the cyclohexylmethyl moiety for the 3,5-AB-CHMFUPPYCA isomer, even at low energies, which was not the case for its 5,3-counterpart. For this reason, the pyrolytic stability of both compounds was assessed to account for thermolytic ‘metabolite’ formation during smoking. However, no pronounced difference in the pyrolytic stability between the two regioisomers could be observed. Three and four ‘metabolites’ were detected in the smoke condensates, respectively (Supplemental Figure S3). In both cases the main pyrolytic degradation product was the primary amide cleavage product (~ 3 %), which was identified as one of the metabolites as well. Similar reactions were observed for other valinamide containing synthetic cannabinoids like e.g. AB-CHMINACA^[12]. Although uptake of these metabolites via smoke might most probably not contribute much to the overall *in vivo* metabolite findings they could lead to problems when interpreting hair analysis results, as ‘metabolite’ findings of chemically labile compounds caused by smoke condensed on hair could be misinterpreted as a proof of consumption.

In summary, metabolic patterns of both AB-CHMFUPPYCA isomers were qualitatively similar. Oxidation of the cyclohexylmethyl side chain was the dominant metabolic reaction. The presented data suggest monohydroxylated metabolites (Figures 2 and 3) as suitable targets for urine analysis. For differentiation of the two isomers the characteristic fragment ion m/z 260 of 3,5-AB-CHMFUPPYCA could be useful. 5,3-AB-CHMFUPPYCA was more efficiently transformed by human liver microsomes when compared to the 3,5-isomer. Moreover, cannabinoid receptor binding and activity may differ between the isomers. Comparing the structures to the known CB₁ receptor antagonist Rimonabant, the similarity to the 5,3-isomer could lead to antagonistic activity, making it unattractive as a cannabis alternative. Regarding the thermolytic stability of the isomers, no remarkable difference was observed. Pyrolytic cleavage of the primary amide bond occurred under smoking conditions

leading to approximately 3 % conversion to artefactual ‘metabolites’. This could bias *in vivo* metabolic profiles after smoking and would have to be considered for interpretation of metabolite findings in hair analysis as well.

Declaration of interests

The authors declare no competing financial interests.

Acknowledgements

This publication has been produced with the financial support of the ‘Prevention of and Fight against Crime’ program of the European Commission. (JUST/2013/ISEC/DRUGS/AG/6421)

References

- [1] European information system and database on new drugs, European Monitoring Centre for Drugs and Drug Addiction. <https://ednd.emcdda.europa.eu>, accessed 11.11.2015.
- [2] U. Girreser, P. Rösner, A. Vasilev. Structure elucidation of the designer drug N-(1-amino-3,3-dimethyl-1-oxobutan-2-yl)-1-(5-fluoropentyl)-3-(4-fluorophenyl)-pyrazole-5-carboxamide and the relevance of predicted ¹³C NMR shifts – a case study. *Drug. Test. Anal.* **2015**, doi: 10.1002/dta.1820
- [3] G. McLaughlin, N. Morris, P.V. Kavanagh, J.D. Power, B. Twamley, J. O'Brien, et al. The synthesis and characterization of the ‘research chemical’ N-(1-amino-3-methyl-1-oxobutan-2-yl)-1-(cyclohexylmethyl)-3-(4-fluorophenyl)-1H-pyrazole-5-carboxamide (3,5-AB-CHMFUPPYCA) and differentiation from its 5,3-regioisomer. *Drug. Test. Anal.* **2015**, doi: 10.1002/dta.1864
- [4] N. Uchiyama, K. Asakawa, R. Kikura-Hanajiri, T. Tsutsumi, T. Hakamatsuka. A new pyrazole-carboxamide type synthetic cannabinoid AB-CHFUPYCA [N-(1-amino-3-methyl-1-oxobutan-2-yl)-1-(cyclohexylmethyl)-3-(4-fluorophenyl)-1H-pyrazole-5-carboxamide] identified in illegal products. *Forensic Toxicol.* **2015**, *33*, 367.
- [5] J.W. Huffman, L.W. Padgett, M.L. Isherwood, J.L. Wiley, B.R. Martin. 1-Alkyl-2-aryl-4-(1-naphthoyl)pyrroles: New high affinity ligands for the cannabinoid CB1 and CB2 receptors. *Bioorg. Med. Chem. Lett.* **2006**, *16*, 5432.
- [6] M. Hutter, S. Broecker, S. Kneisel, V. Auwärter. Identification of the major urinary metabolites in man of seven synthetic cannabinoids of the aminoalkylindole type present as adulterants in ‘herbal mixtures’ using LC-MS/MS techniques. *J. Mass Spectrom.* **2012**, *47*, 54.
- [7] T. Berg, L. Kaur, A. Risnes, S.M. Havig, R. Karinen. Determination of a selection of synthetic cannabinoids and metabolites in urine by UHPSFC-MS/MS and by UHPLC-MS/MS. *Drug. Test. Anal.* **2015**, doi: 10.1002/dta.1844
- [8] N.B. Holm, A.J. Pedersen, P.W. Dalsgaard, K. Linnet. Metabolites of 5F-AKB-48, a synthetic cannabinoid receptor agonist, identified in human urine and liver microsomal preparations using liquid chromatography high-resolution mass spectrometry. *Drug. Test. Anal.* **2015**, *7*, 199.
- [9] T. Sobolevsky, I. Prasolov, G. Rodchenkov. Detection of urinary metabolites of AM-2201 and UR-144, two novel synthetic cannabinoids. *Drug. Test. Anal.* **2012**, *4*, 745.
- [10] M. Hutter, B. Moosmann, S. Kneisel, V. Auwärter. Characteristics of the designer drug and synthetic cannabinoid receptor agonist AM-2201 regarding its chemistry and metabolism. *J. Mass Spectrom.* **2013**, *48*, 885.

- [11] B. Moosmann, V. Angerer, V. Auwärter. Inhomogeneities in herbal mixtures: a serious risk for consumers. *Forensic Toxicol.* **2015**, *33*, 54.
- [12] F. Franz, V. Angerer, M. Hermanns-Clausen, B. Moosmann, V. Auwärter. Metabolites of synthetic cannabinoids in hair – proof of consumption or false friends for interpretation?. 53rd Annual meeting of the International Association of Forensic Toxicologists (TIAFT), Florence, 30.08. – 04.09.**2015**

Table 1. Identified metabolites of 3,5-AB-CHMFUPPYCA after 1h incubation with pooled human liver microsomes (pHLM) in the order of their retention time (RT). All determinations were performed in triplicate. For the ranking the mean area ratios between the metabolite and the most abundant metabolite (A08) was used and relative standard deviations (RSD) are given. The four most abundant metabolites are highlighted in bold type. Biotransformation sites: Cyclohexylmethyl (CHM) or valinamide (VA) moiety.

ID	Biotransformation	Site	RT [min]	Formula	<i>m/z</i> [Da]	Major fragment ions [Da]	Area ratio	RSD	Rank
---	3,5-AB-CHMFUPPYCA	---	18.3	C ₂₂ H ₃₀ FN ₄ O ₂	401	189, 260, 356	---	---	---
A01	Dihydroxylation	CHM + VA	6.5	C ₂₂ H ₃₀ FN ₄ O ₄	433	189, 258, 276, 370	3.0%	8.4%	12
A02	Dihydroxylation	CHM	7.2	C ₂₂ H ₃₀ FN ₄ O ₄	433	189, 260, 415	2.2%	16.7%	16
A03	Dihydroxylation	CHM + VA	7.3	C ₂₂ H ₃₀ FN ₄ O ₄	433	189, 258, 276, 415	3.3%	10.0%	11
A04	Dihydroxylation	CHM + VA	7.7	C ₂₂ H ₃₀ FN ₄ O ₄	433	189, 258, 276, 283	4.2%	3.9%	10
A05	Hydroxylation + ketone	CHM	7.8	C ₂₂ H ₂₈ FN ₄ O ₄	431	189, 260, 327, 386, 415	1.1%	9.2%	21
A06	Dihydroxylation	CHM	8.2	C ₂₂ H ₃₀ FN ₄ O ₄	433	189, 260, 415	1.3%	6.9%	18
A07	Dihydroxylation	CHM	8.4	C ₂₂ H ₃₀ FN ₄ O ₄	433	189, 260, 352, 415	1.1%	4.1%	20
A08	Hydroxylation	CHM	9.0	C₂₂H₃₀FN₄O₃	417	189, 260, 372	100.0%	0.0%	1
A09	Hydroxylation	CHM	9.6	C₂₂H₃₀FN₄O₃	417	189, 260, 283, 354, 382, 399	39.9%	4.0%	4
A10	Hydroxylation	CHM	9.8	C₂₂H₃₀FN₄O₃	417	189, 260, 283, 354, 382, 399	71.5%	0.3%	3
A11	Hydroxylation	CHM	10.2	C₂₂H₃₀FN₄O₃	417	189, 260, 283, 354, 382, 399	82.8%	2.4%	2
A12	Ketone	CHM	10.4	C ₂₂ H ₂₈ FN ₄ O ₃	415	189, 299, 370, 398	6.6%	8.9%	8
A13	Ketone	CHM	10.9	C ₂₂ H ₂₈ FN ₄ O ₃	415	189, 260, 370, 398	32.2%	12.6%	6
A14	Hydroxylation	CHM	11.9	C ₂₂ H ₃₀ FN ₄ O ₃	417	189, 260, 283, 354, 382, 399	1.2%	5.5%	19
A15	Hydroxylation + hydrolysis	CHM + VA	12.1	C ₂₂ H ₂₉ FN ₃ O ₄	418	189, 260, 400	0.3%	11.1%	22
A16	Hydroxylation	CHM	13.1	C ₂₂ H ₃₀ FN ₄ O ₃	417	189, 260, 283, 354, 382, 399	2.7%	5.3%	13
A17	Dihydroxylation	VA	13.3	C ₂₂ H ₃₀ FN ₄ O ₄	433	189, 246, 274, 302, 388, 416	1.6%	5.6%	17
A18	Hydroxylation	CHM	13.8	C ₂₂ H ₃₀ FN ₄ O ₃	417	189, 260, 283, 354, 382, 399	5.7%	11.8%	9
A19	Hydroxylation	VA	15.1	C ₂₂ H ₃₀ FN ₄ O ₃	417	189, 258, 276, 372	39.3%	16.4%	5
A20	Dehydrogenation	CHM	17.0	C ₂₂ H ₂₈ FN ₄ O ₂	399	189, 260, 354	2.5%	19.8%	14
A21	Dehydrogenation	VA	18.1	C ₂₂ H ₂₈ FN ₄ O ₂	399	189, 258, 354	11.4%	16.8%	7
A22	Hydrolysis	VA	20.5	C ₂₂ H ₂₉ FN ₃ O ₃	402	189, 260, 385	2.3%	4.1%	15

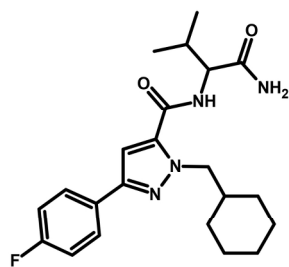
Table 2. Identified metabolites of 5,3-AB-CHMFUPPYCA after 1h incubation with pooled human liver microsomes (pHLM) in the order of their retention time (RT). All determinations were performed in triplicate. For the ranking the mean area ratios between the metabolite and the most abundant metabolite (B06) was used and relative standard deviations (RSD) are given. The four most abundant metabolites are highlighted in bold type. Biotransformation sites: Cyclohexylmethyl (CHM) or valinamide (VA) moiety.

ID	Type	Site	RT [min]	Formula	<i>m/z</i> [Da]	Major fragment ions [Da]	Area ratio	RSD	Rank
---	5,3-AB-CHMFUPPYCA	---	17.3	C ₂₂ H ₃₀ FN ₄ O ₂	401	189, 285, 356, 384	---	---	---
B01	Dihydroxylation	CHM + VA	6	C ₂₂ H ₃₀ FN ₄ O ₄	433	189, 301, 370, 388, 416	11.0%	13.7%	6
B02	Hydroxylation + ketone	CHM	6.2	C ₂₂ H ₂₈ FN ₄ O ₄	431	189, 315, 327, 386, 414	0.7%	23.5%	21
B03	Hydroxylation + ketone	CHM + VA	7	C ₂₂ H ₂₈ FN ₄ O ₄	431	189, 299, 368, 386, 396, 414	1.4%	25.9%	16
B04	Dihydroxylation	CHM + VA	7.4	C ₂₂ H ₃₀ FN ₄ O ₄	433	189, 301, 370, 388, 416	2.4%	10.7%	13
B05	Hydroxylation + dehydrogenation	CHM + VA	7.8	C ₂₂ H ₂₈ FN ₄ O ₃	415	189, 301, 370, 398	1.2%	18.6%	19
B06	Hydroxylation	CHM	8	C₂₂H₃₀FN₄O₃	417	189, 301, 354, 372, 400	100.0%	0.0%	1
B07	Hydroxylation	CHM	8.2	C ₂₂ H ₃₀ FN ₄ O ₃	417	189, 283, 301, 354, 372, 400	9.4%	2.5%	8
B08	Hydroxylation	CHM	8.5	C₂₂H₃₀FN₄O₃	417	189, 283, 301, 354, 372, 400	19.4%	1.8%	4
B09	Hydroxylation	CHM	8.6	C ₂₂ H ₃₀ FN ₄ O ₃	417	189, 283, 301, 354, 372, 400	13.3%	5.5%	5
B10	Ketone	CHM	8.9	C ₂₂ H ₂₈ FN ₄ O ₃	415	189, 299, 370, 398	2.8%	5.8%	12
B11	Hydroxylation	CHM	9.3	C ₂₂ H ₃₀ FN ₄ O ₃	417	189, 301, 354, 372, 400	4.6%	3.8%	10
B12	Ketone	CHM	9.3	C₂₂H₂₈FN₄O₃	415	189, 299, 370, 398	19.8%	23.7%	3
B13	Hydroxylation	CHM	9.7	C₂₂H₃₀FN₄O₃	417	189, 301, 354, 372, 400	27.4%	3.6%	2
B14	Hydroxylation + hydrolysis	CHM	9.9	C ₂₂ H ₂₉ FN ₃ O ₄	418	189, 283, 301, 372, 400	2.1%	27.2%	14
B15	Hydroxylation	CHM	10.6	C ₂₂ H ₃₀ FN ₄ O ₃	417	189, 301, 372, 400	1.2%	3.6%	18
B16	Hydroxylation	CHM	11.8	C ₂₂ H ₃₀ FN ₄ O ₃	417	189, 260, 301, 354, 372, 400	1.3%	5.9%	17
B17	Dihydroxylation	VA	12.9	C ₂₂ H ₃₀ FN ₄ O ₄	433	189, 285, 416	0.8%	19.1%	20
B18	Hydroxylation	VA	13.1	C ₂₂ H ₃₀ FN ₄ O ₃	417	189, 285, 400	5.6%	10.1%	9
B19	Hydroxylation	VA	14.3	C ₂₂ H ₃₀ FN ₄ O ₃	417	189, 285, 354, 372, 400	10.9%	6.9%	7
B20	Hydrolysis (secondary amide)	VA	15.5	C ₁₇ H ₂₀ FN ₂ O ₂	303	189, 285	0.3%	12.7%	23
B21	Dehydrogenation	CHM	15.7	C ₂₂ H ₂₈ FN ₄ O ₂	399	189, 283, 354	0.5%	15.1%	22
B22	Dehydrogenation	VA	17.1	C ₂₂ H ₂₈ FN ₄ O ₂	399	189, 285, 354, 382	1.5%	21.6%	15
B23	Hydrolysis (primary amide)	CHM	19.6	C ₂₂ H ₂₉ FN ₃ O ₃	402	189, 285, 356	3.4%	1.2%	11

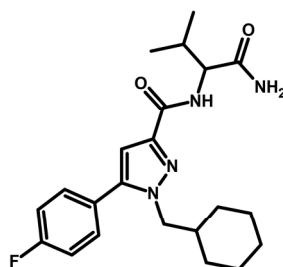
Figure 1. Molecular structures of the novel pyrazole compounds in comparison to JHW-307 and Rimonabant.

Figure 2. Enhanced product ion scans recorded using a collision energy of 35 V with a spread of 15 V of the four most abundant metabolites (A08, A09, A10, A11) identified after 1h incubation of 3,5-AB-CHMFUPPYCA with pooled human liver microsomes and proposed fragmentation.

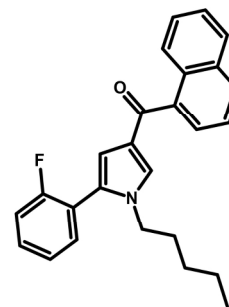
Figure 3. Enhanced product ion scans recorded using a collision energy of 35 V with a spread of 15 V of the four most abundant metabolites (B06, B08, B12, B13) identified after 1h incubation of 5,3-AB-CHMFUPPYCA with pooled human liver microsomes and proposed fragmentation.



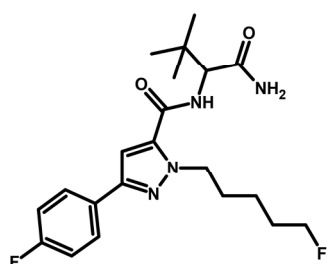
3,5-AB-CHMFUPPYCA



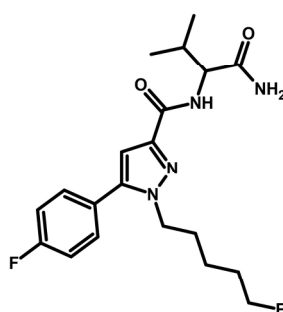
5,3-AB-CHMFUPPYCA



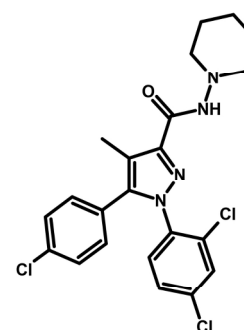
JWH-307



3,5-5F-ADB-FUPPYCA



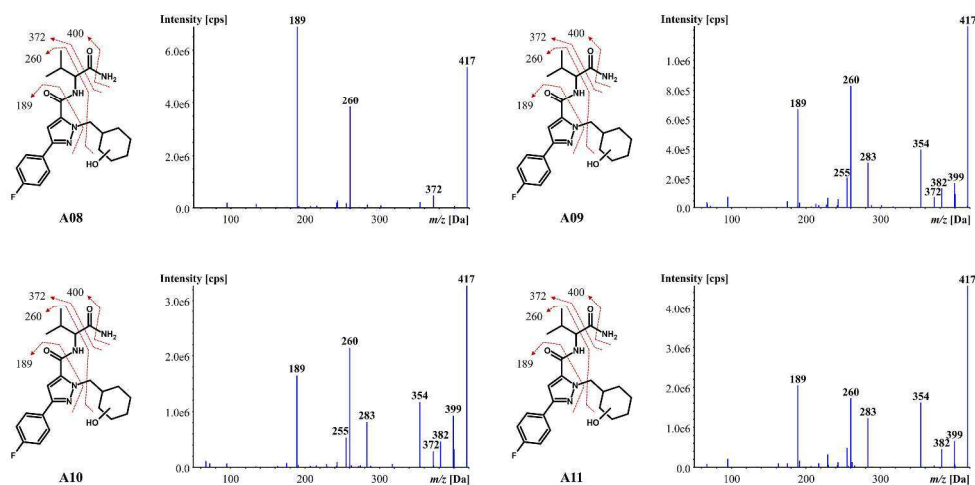
5,3-5F-AB-FUPPYCA (AZ-037)



Rimonabant

Molecule structures of the novel pyrazole compounds in comparison to JWH-307 and Rimonabant.

190x142mm (300 x 300 DPI)



Enhanced product ion scans recorded using a collision energy of 35 V with a spread of 15 V of the four most abundant metabolites (A08, A09, A10, A11) identified after 1h incubation of 3,5-AB-CHMFUPPYCA with pooled human liver microsomes and proposed fragmentation.
508x264mm (300 x 300 DPI)